Technical Notes

Experimental Results in High-Specific-Impulse Thermo-Ionic Acceleration

ADRIANO C. DUCATI,* GABRIEL M. GIANNINI,† AND ERICH MUEHLBERGER‡
Giannini Scientific Corporation, Santa Ana, Calif.

THE term "thermo-ionic acceleration" is used to define the field of electrothermal acceleration using highly ionized gases. The concept involves the ability to produce a very high propellant temperature and the abandonment of attempts to recover the major part of the energy stored in dissociation and ionization of the propellant. Attempts to control with conventional nozzles the greater part of the undirected energy of the thermally accelerated plasma stream are no longer pursued. Electromagnetic effects are increased due to the high value of ionization and currents, and these effects contribute to the acceleration and high-temperature containment. The result of this procedure is to reduce the physical dimensions of the accelerating mechanism and the internal operating pressure. In so doing, temperatures and velocities, previously considered unattainable, have been reached with an exceptional increase in the values of specific impulse and efficiency.

The "thermo-ionic" thrustor differs from a conventional arcjet by operating at a low gas density, high current, and very high level of ionization. In addition, it appears that self-induced magnetic effects help to contain and accelerate the plasma.

Using hydrogen as a propellant, specific impulse values in excess of 10,000 sec (corresponding to an exhaust velocity of approximately 60 miles/sec) have been achieved. Although the flow-accelerating mechanisms of this thrustor are not yet completely understood, research work is progressing in both the analytical and experimental phases. Based on experimental results, it is believed that the thermo-ionic thrustor can attain specific impulse values approaching 20,000 sec and thrust density values of over 200 psf (of thrusting area).

The thermo-ionic thrustor retains the arcjet engine's advantages of beam neutralization, comparatively high thrust, simple power-conditioning requirements, and compact size. In addition, it can operate at constant thrust or variable thrust at constant specific impulse by changing the electrical power input and propellant flow rate. Similarly, specific impulse can be varied by changing the power input at a constant propellant flow rate or by varying the flow rate at constant power. A variation of thrust up to 10 to 1 has been achieved to date.

The simulation capability of this thermo-ionic technology may be equally important and have a more immediate application potential. The highly ionized, high-temperature, low-density exhaust from this accelerator could be extremely valuable in simulating the thermodynamic conditions of a hot hydrogen core in a gaseous-core nuclear-fission reactor. Another use for a simulator using this device would be in the development of MHD electrical power generation equipment.

Experimental tests have been carried out using a water-cooled plasma generator with hydrogen propellant. Table 1 presents the numerical test results from early experiments conducted in 1963. The first column lists the specific impulse values obtained. The second column indicates the total electrical input power into the thrustor. The third column shows the energy content of the expelled propellant, and the fourth column shows the measured thrust. The next three columns present the various efficiencies. The first efficiency, η^{eg}, is the ratio of the energy in the expelled gas to the total electrical energy; the second efficiency, η^{gk}, is the ratio of the required theoretical energy to the energy content of the expelled propellant mass flow; and the third efficiency, η^{ek}, is the ratio of the required theoretical energy to the total electrical input energy. The last column presents the stagnation enthalpy of the propellant.

In most electrothermal propulsors, a thermodynamic nozzle is used. Inherent losses in the nozzle (thermal, friction, radiation, undirected flow, etc.) account for a considerable

Table 1 Experimental test results obtained with a water-cooled electrothermal plasma generator using hydrogen propellant (December 1963)[a]

I_{sp}, sec	Input, kw	Gas, kw	Thrust, g	η^{eg}, %	η^{gk}, %	η^{ek}, %	Stagnation enthalpy, cal/g
3,080	71	51	77	68	22	15	486,000
3,440	78	54	86	69	26	18	514,000
3,720	85	59	93	70	28	19	564,000
4,070	97	70	102	72	28	21	670,000
4,200	103	71	105	70	29	20	678,000
4,600	115	83	115	72	30	21	791,000
4,870	131	84	122	64	33	21	800,000
5,150	136	86	129	63	37	24	822,000
6,900	178	120	172	68	46	32	1,142,000
7,200	190	128	180	68	49	33	1,217,000
8,000	204	140	200	69	56	38	1,333,000
9,000	224	155	225	68	62	43	1,477,000
10,000	260	176	250	68	67	46	1,680,000

[a] Mass flow H_2 = 0.025 g/sec.

Received May 26, 1964. This work was supported by the Air Force Office of Scientific Research under AFOSR Contract AF 49(638)-1161. The authors wish to thank Hendricus Loos and Richard P. Treat for important discussions.

* Director, Special Projects Group. Member AIAA.
† President. Associate Fellow Member AIAA.
‡ Research Engineer. Member AIAA.

Table 2 "Forecast" of thermo-ionic propulsion progress (data extrapolated from actual experimental results with hydrogen propellant at I_{sp} 10,000 sec and mass flow = 0.025 g/sec, η^{eg} increased to 90%)

I_{sp}, sec	Input, kw	Gas, kw	Thrust, g	η^{eg}, %	η^{gk}, %	η^{ek}, %	Stagnation enthalpy, cal/g
10,000	196	177	250	90	69	63	1,685,000
11,000	218	196	275	90	74	67	1,867,000
12,000	252	227	300	90	77	69	2,166,000
13,000	283	255	325	90	79	71	2,430,000
14,000	328	296	350	90	81	73	2,820,000
15,000	360	325	375	90	83	75	3,095,000
16,000	400	360	400	90	85	77	3,420,000
17,000	444	400	425	90	87	79	3,805,000
18,000	485	437	450	90	89	81	4,167,000
19,000	528	478	475	90	91	83	4,550,000
20,000	580	522	500	90	93	85	4,970,000

portion of the losses, and there seems to be no practical means of changing this appreciably. Attempts to recover the energy stored in dissociation or ionization by recombination also seem very difficult because of the velocity of the gases and the practical length of such a nozzle. Other problems, of course, include the limitation of attainable specific impulse to that resulting in the nozzle erosion. For this reason, the conventional nozzle has been nearly eliminated, allowing the attainment of higher temperatures and extremely high stagnation enthalpies.

Specific impulses higher than 10,000 sec have been measured. The stagnation temperature corresponding to 10,000 sec is over 100,000°K. Now, if one assumes that kinetic pressure forces are entirely responsible for the acceleration of the flow, it implies that static temperatures exist in the arc in the order of 100,000°K. Since we know that temperatures on the electrode surfaces are not much over 3000°K, there must be very large temperature gradients in the arc. This raises the question of whether such high temperatures and large temperature gradients actually exist in the arc or if magnetic forces are contributing to the acceleration of the flow. The existence of such forces would permit lower static temperatures for the same stagnation temperature in the expanded flow. The experimental results shown in Fig. 1 seem to confirm the presence of an appreciable magnetic effect.

In the region of the arc, where the flow is heated and accelerated, the gas is a good electrical conductor. Thus, magnetic forces could be significant in the acceleration of the flow if the magnetic pressure is comparable to the gas kinetic pressure. The highest specific impulses have been obtained at currents of over 3000 amp with chamber pressure under 0.10 atm. The self-magnetic field corresponding to 3000 amp and to the estimated arc diameter gives a magnetic pressure $B^2/2\mu_0$ comparable to 0.10 atm. It should be noted that the presence of large magnetic forces does not necessarily imply that these forces are effective in accelerating the flow.

Magnetic forces may be important in determining the structure of the arc as in the confinement of a current filament by its self-magnetic field. The steady-state solution of the macroscopic equations of a self-pinched, fully ionized, infinite, cylindrical plasma shows that

$$2NkT = I^2 \tag{1}$$

where N is the number density of electrons and ions per unit length along the axis of the plasma cylinder, T is the mean temperature of electrons and ions, I is the total current, and k is Boltzmann's constant. To obtain the result (1), it is assumed that the temperature in the plasma is constant and that the plasma is confined within a finite cross section. Dividing (1) by the cross-sectional area A gives

$$2p = I^2/A \tag{2}$$

where $p = NkT/A$ can be interpreted as an average pressure of the plasma. From (2) we see that, if the current is kept constant, a decrease in the average kinetic pressure in a self-pinched plasma results in an increased area. Rough observations on the arc have shown that its diameter increases as the arc chamber pressure is reduced. This qualitative agreement of the dependence of arc diameter on pressure does not imply that magnetic forces determine the arc diameter, since the diameter of the positive column of an arc discharge also increases as pressure is decreased when magnetic forces are not dominant.

Another important development that contributes basically to the behavior of the thermo-ionic operation is the establishment of conditions where a large part of the cathode is participating in the discharge. Visual observation shows the whole tip of the cathode glowing uniformly rather than the usual small diameter spot moving on the cathode surface. This type of behavior at the cathode is important, for it decreases the current density, permitting an increase in the total current of the arc, and is probably a significant factor

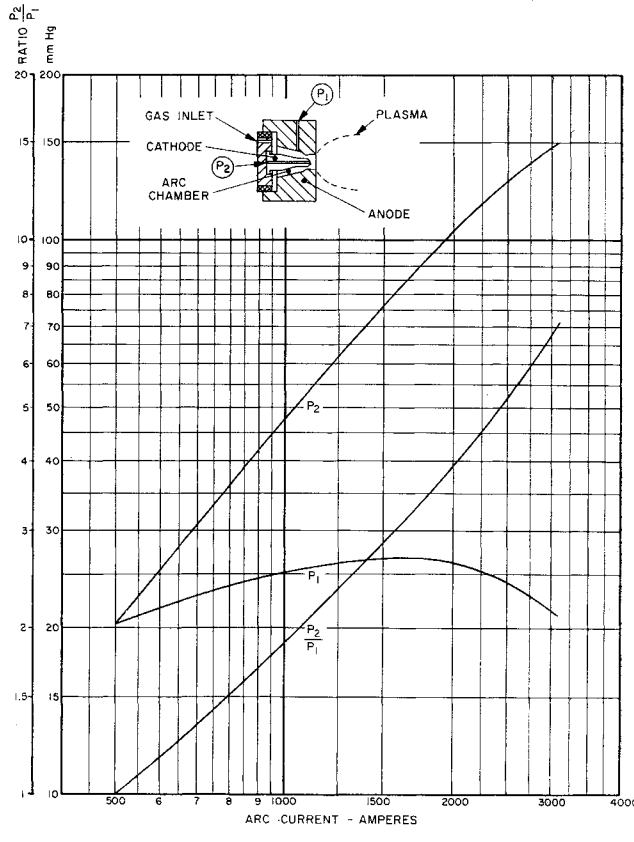

Fig. 1 Variation of pressure with increasing current.

in preventing the cathode from melting at extremely high currents. It should be noted that a high degree of ionization is the principal characteristic of the hydrogen propellant in the temperature range involved. Also, the gas is in the neutral plasma state at all times. Since the main species of the frozen flow are protons and electrons, perfect-gas thermodynamic conditions are approached.

The interesting phenomena described open up a new field of possibilities for thermo-ionic acceleration. Table 2 is a forecast of the results obtainable if the heat-transfer efficiency can be increased from 70 to 90% and specific impulses higher than 10,000 sec are attained. This is the scope of the future work.

Space Station Design Parameter Effects on Artificial g Field

CARL A. LARSON*
General Electric Company, Huntsville, Ala.

Nomenclature

x, y, z	=	axes attached and rotating with the space station, such that z is the spin axis
A, B, C	=	principal moments of inertia about the x, y, z axes, respectively
$\mathbf{w}$	=	spin vector
p, q, r	=	components of the spin vector about the x, y, z axes, respectively
$\mathbf{i}, \mathbf{j}, \mathbf{k}$	=	unit vectors directed along the x, y, z axes, respectively
0	=	subscript denoting initial value of a parameter
k_1	=	$[(C - B)/A]r_0$
k_2	=	$[(C - A)/B]r_0$
K	=	$(k_1k_2)^{1/2}/r_0$

THE main purpose for rotating a manned space station is to provide a simulated gravity field that is habitable by man, i.e., a field whose magnitude and directional changes are kept within the physiological tolerance limits of the man. A man on board a rotating space station may have his vestibular system stimulated in two different ways: 1) by normal head movements in the conduction of his tasks or 2) by disturbed motion of the space station which causes it to rotate simultaneously about two or more of its axes. The purpose of this investigation is to point out the effects imposed by the latter condition on the artificial gravity field.

For a configuration rotating in a passive state (no energy inputs), the gravity field acting on a man positioned along the x axis is given by

$$n\mathbf{g} = -\dot{\mathbf{w}} \times \mathbf{r} - \mathbf{w}\,x(\mathbf{w} \times \mathbf{r}) = x[\mathbf{i}(q^2 + r^2) - \mathbf{j}(pq + \dot{r}) - \mathbf{k}(pr - \dot{q})] \quad (1)$$

Equation (1) assumes that energy dissipation can exist in the absence of external torques, and therefore the only stable condition for a rotating system is rotation about the axis of maximum moment of inertia. The disturbed motion of this type of configuration, which has its moments of inertia related by $C > B > A$, is not readily described, because the equations of motion (Euler's dynamic equations) are not directly integrable. Hence, the polhode cone and trace on the inertia ellipsoid which describes this motion[1] must be looked at in more detail. The polhode cone and its trace in the xz plane are shown in Fig. 1.

It is noted that the major factor causing the trace to be distorted in the xz plane is the variance in spin velocity r, which results from the energy coupled from about the other

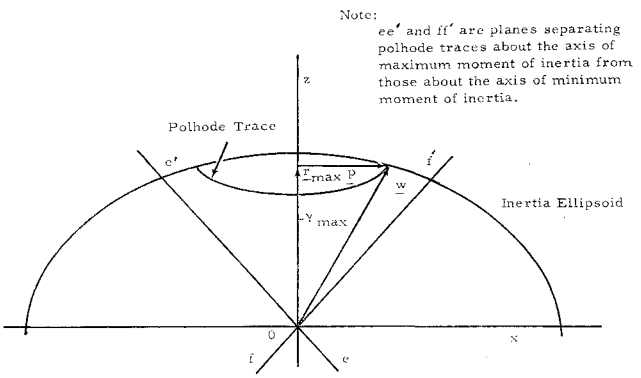

Fig. 1 Polhode trace in the xz plane.

axes. To analyze this variance, the equation of the trace in this plane is examined. It is given by

$$A(A - B)p^2 + C(C - B)r^2 = L^2 \quad (2)$$

From Fig. 1, it is seen that p can be expressed as a function of the spin velocity r by

$$p = r \tan\gamma \quad (3)$$

Then Eq. (2) can be rewritten as

$$A(A - B)r^2 \tan^2\gamma + C(C - B)r^2 = L^2$$

or

$$r = L[C(C - B) - A(B - A)\tan^2\gamma]^{-1/2} \quad (4)$$

Referring to Fig. 1 again, it is noted that, in the motion of the $\mathbf{w}$ vector about the z axis, the maximum angle swept out in the xz plane is γ; hence, this angle is directly related to the size of the polhode cones about the z axis. Using this relationship, the variance in r can be calculated with respect to the mean value of r during a rotation of $\mathbf{w}$ by the following expression:

$$r\% = [(r - r_0)/(r + r_0)]100 \quad (5)$$

where r is the spin velocity at γ_{max} and r_0 the spin velocity at $\gamma = 0$

Considering several types of configurations, a plot of percent variation of r with γ is determined and presented in Fig. 2. For these configurations, it is seen that for small disturbances ($\gamma \leq 7°$) there is less than a 1% variation in the spin velocity r. Hence, for small disturbances the equations of motion for the $C > B > A$ configuration can be written, in general, as

$$\left.\begin{aligned} A\dot{p} + (C - B)qr &= 0 \\ B\dot{q} + (A - C)pr &= 0 \\ r &= r_0 \end{aligned}\right\} \quad (6)$$

The solutions of Eqs. (6) become

$$\begin{aligned} p &= p_0 \cos Kr_0t - (k_1/Kr_0)q_0 \sin Kr_0t \\ q &= q_0 \cos Kr_0t + (k_2/Kr_0)p_0 \sin Kr_0t \\ r &= r_0 \end{aligned} \quad (7)$$

Substituting the values for p, q, and r as derived in Eq. (7) into Eq. (1) gives

$$\begin{aligned} n\mathbf{g} = x\{&\mathbf{i}[q_0^2 \cos^2 Kr_0t + \tfrac{1}{2}(k_2/k_1)^{1/2}p_0q_0 \sin 2Kr_0t + (k_2/k_1)p_0^2 \sin^2 Kr_0t + r_0^2] - \mathbf{j}[-\tfrac{1}{2}(k_1/k_2)^{1/2}q_0^2 \sin 2Kr_0t + p_0q_0(\cos^2 Kr_0t - \sin^2 Kr_0t) + \tfrac{1}{2}(k_2/k_1)^{1/2}p_0^2 \sin 2Kr_0t] - \\ &\mathbf{k}[(1 - k_2/r_0)p_0r_0 \cos Kr_0t - (k_1/k_2)^{1/2}(1 - k_2/r_0)q_0r_0 \sin Kr_0t]\} \end{aligned} \quad (8)$$

Received January 2, 1963; revision received July 15, 1963.
* Engineer, Apollo Support Department.